# Highly Accelerated Parallel Imaging Using Rotating Radiofrequency Coil Array at 7T

Mingyan Li[1], Jin Jin[1], Feng Liu[1], Adnan Trakic[1], Ewald Weber[1], and Stuart Crozier[1]

[1]*School of Information Technology and Electrical Engineering, The University of Queensland, Brisbane, Queensland, Australia*

**Introduction:** Previous studies have shown that the approach of sensitivity encoding using a mechanically rotating radiofrequency coil (RRFC) is capable of emulating a large number of decoupled coil elements [1, 2]. Recently, the RRFC concept has been successfully combined with phased-array coil (PACs) techniques to further improve the sensitivity encoding capability, using a naturally-decoupled RF coil array. A novel 4-element RRFC array (RRFCA) has shown to have better imaging acceleration capability than PACs with twice as many coil elements at 3T [3]. An enhanced acceleration capability of RRFCA is expected at higher fields as two advantages of the RRFCA can be strengthened: (1) the mutual coupling between RRFCA elements is dramatically reduced due to the shorter RF wavelength and (2) the $B_1$ field (sensitivity profiles) become more inhomogeneous, which has the potential to improve encoding capability. In this novel study, the potential of RRFCA to accelerate imaging at 7T was investigated. A 4-element RRFCA in different operating modes was compared with an 8-element stationary PACs at various reduction factors.

**Method:** The RRFCA consists of 4 identical coil elements evenly distributed around the cylindrical coil former of 280 mm in diameter. The length of each coil is 170 mm (longitudinal) with a subtended angle of 35˚. This arrangement naturally endows the excellent electromagnetic isolation between any two coil elements. After loading a 250 mm diameter homogeneous spherical phantom with $\varepsilon_r$=50.5 and σ=0.65 S/m (average of brain tissue at 300 MHz), all the mutual couplings are under -31dB without using any decoupling circuitry. This is much improved compared with -15dB mutual coupling of RRFCA elements at 3T. The RRFCA and phantom geometry are shown in Fig.1. The modelling and electromagnetic solutions were performed with the commercially available software package FEKO (EMSS, SA). The circular polarization of steady-state RF magnetic field ($B_1$) was calculated according to [4].

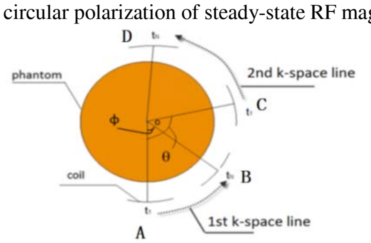


Fig. 2 Illustration of operation mode and optimisation method in fast-mode. In stepping-mode, φ=0

In previous works [1-3], the RRFC was actuated pneumatically and rotated about the subject with constant velocity in fast-mode (typically over 1500rpm). Since the acquisition time ($T_{ACQ}$) is comparable to the rotational period, within the time of sampling each *k*-space line, acquisition experiences time-varying sensitivity profiles as shown in Fig. 2 from point A to B and C to D. However, fast rotating may bring multiple practical issues, which can be avoided by actuating RRFCA with a non-magnetic motor. In this way, the RRFCA sample at certain points (φ=0) in a stepped fashion with precise position-control, such as at point A and C. Compared with conventional PACs, the RRFCA provides the ability of encoding with much larger number of sensitivity profiles, in both fast- and stepping- modes.

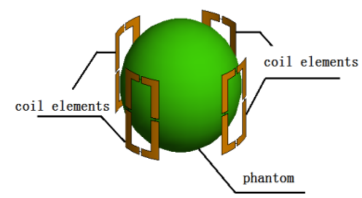


Fig. 1 RRFCA and phantom geometry (natural decoupling (-31 dB))

The fast-mode provides us additional capability of optimising the sensitivity encoding performance, by adjusting the rotating speed ($\omega$) in relation to the imaging parameters, such as repetition time (*TR*) and $T_{ACQ}$. The optimal speed of revolution can be obtained as following functions in Fast Low Angle Shot (FLASH) imaging sequence:

$$\underset{\theta(\omega),\varphi(\omega)}{\operatorname{argmin}}\left\{\sqrt{\frac{\sum_{x=1}^{N}\sum_{y=1}^{N}(g_{x,y}-1)^2}{N^2}}\right\} \quad (1)\text{, where } \theta(\omega)=TR\times\omega\backslash 2\pi \quad (2) \quad \text{and } \varphi(\omega)=T_{Acq}\times\omega \quad (3)$$

The operator '\' takes the remainder of the division; $g_{xy}$ is the calculated g-map [5] taking into account the time-varying sensitivity; $\theta$ denotes angular displacement during *TR*; and $\varphi$ indicates the angular displacement during $T_{ACQ}$. In essence, Eq.(1) minimises the g-map of a parallel imaging experiment and thereby improves acceleration capability. Although having the ability to optimise the acceleration performance, the fast-mode has multiple practical issues, including the need to solve a very large set of simultaneous equations in calculating g-map for optimisation and in recovering the image. In stepping-mode instead, the RRFCA is through a number of discrete equidistantly distributed angular positions between adjacent $T_{ACQ}$. Therefore, the RRFCA provides a unique and stationary sensitivity for each $T_{ACQ}$ ($\varphi$=0). For Cartesian sampling, the image can be recovered straightforwardly in a fashion similar to SENSE [5], while assigning the corresponding sensitivity profiles to each *k*-space line.

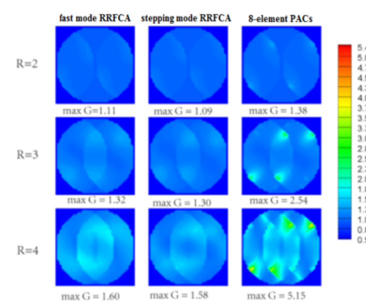


Fig. 3 g-maps comparison under different reduction factors for RRFCA and 8-elements PACs

**Results and Discussions:** Fig. 3 shows the g-maps of different reduction factors for RRFCA working in fast- and stepping-mode, and the 8-element PACs. It can be seen that, the stepping-mode RRFCA has similar acceleration ability as the fast-mode RRFCA. At R=4, the max g-factor for the fast- and stepping-mode are 1.6 and 1.58, respectively. However, the mechanical motor actuated motion makes the stepping-mode RRFCA a more practical approach. Under all reduction factors, the RRFCA has clear advantages in terms of g-map and max g-factor. When R=4, the max g-factor for 8-element PACs is 5.15, making it infeasible for imaging applications. Comparing to the RRFCA at 3 T [3] (max g-factor = 2.4 when R = 4), the higher static magnetic field provided enhanced encoding capability. It can be seen from Fig. 4 that, RRFCA provides excellent image reconstruction that is free from aliasing artefacts, which are typically seen in conventional PACs imaging with high accelerations (Fig.5 right). Compared with the PACs reconstruction, the errors produced by RRFCA are smeared more uniformly within the image, which is consistent with the g-map calculation. The root-mean-square-deviation (RMSD) and artefact power (AP) of RRFCA (RMSD: 0.016 and AP: 0.0018) are much improved compared with the stationary 8-element PACs (RMSD: 0.0241 and AP: 0.0034).

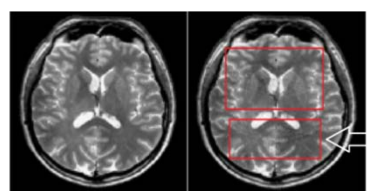

Fig. 4 Reconstructed images by RRFCA (left) and 8-element PACs (right) when R=4

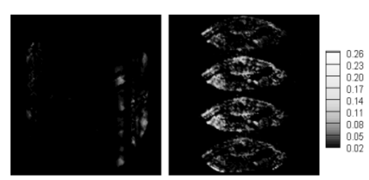


Fig. 5 Error maps of RRFCA (left) and 8-element PACs (right)

**Conclusion:** The acceleration ability of the novel rotating array is strengthened at 7 T when compared with lower field strengths, owing to the improved electromagnetic isolation and more distinctive sensitivity profiles. The calculated g-maps and reconstructed images indicate that the 4-element RRFCA has clear advantages over conventional 8-element stationary PACs.

**References:** [1] A.Trakic, et al, *Concepts in Magn Reson Part B:* vol. 35B, 2009 [2] A.Trakic, et al, *JMR*,vol 201,2009. [3] M. Li, et al, 1117, *IEEE EMBC* 2012 [4] D. Hoult, *Concepts in Magn Reson*, vol 12, 2000 [5] K. Pruessmann, et al, *Magn Reson in Med*, vol46, 1999.